3D printed PLA sacrificial honeycomb cladding blast mitigation

H. B. Rebelo[1,2], D. Lecompte[3], C. Cismaşiu[1,4], A. Jonet[3], B. Belkassem[3], A. Maazoun[3,5]
[1] *Civil Engineering Department, FCT-NOVA, Portugal.*
[2] *CINAMIL, Military Academy, Portugal.*
[3] *Civil and Materials Engineering Department, Royal Military Academy, Belgium.*
[4] *CERIS, Portugal.*
[5] *Magnel Laboratory for Concrete Research, Ghent University, Belgium.*

ABSTRACT

The concept of a sacrificial cladding solution emerged in the last decades as a response to the increasing use of improvised explosive devices in terrorist attacks against civil targets. Resorting to the novel 3D printing manufacturing techniques readily available nowadays, the present study examines the nonlinear response of 3D printed PLA honeycomb structures in order to analyse their energy mitigation capacity. These structures are used as the crushable core of a sacrificial cladding solution in combination with an aluminium front plate. The response of the proposed sacrificial solution, when subjected to blast loads, is experimentally determined by means of an explosive driven shock tube, while the corresponding numerical simulations are achieved through the commercial finite element software LS-DYNA. The experimental and numerical results are in good agreement and readily show that, as expected, the plateau force is directly proportional to the considered infill ratios. Additionally, the nonlinear response of PLA honeycomb structures, when subjected to out-of-plane blast loads, was found to be mainly dependent on relative density, which controls the crushing of the top and bottom layers of the PLA honeycomb and the buckling of its interior cell walls.

Keywords: Sacrificial cladding; Explosive Driven Shock Tube (EDST); Fused deposition modelling (FDM); Polyactic acid (PLA); Honeycomb structure.

INTRODUCTION

The implementation of protective solutions is crucial to mitigate the effects of blast loads on structures and to ensure their survivability. Traditionally, strengthening is the commonly used method of protection of structural members. Nonetheless, the concept of sacrificial cladding solution has risen in the interest of the research community [1-6] due to their reduced mass and high energy absorption capacities. They are usually fixed on the exterior of the structural member and are composed by a crushable core and two skin plates. The latter aim to evenly distribute the applied blast pressure to the former and ensure its uniform compression. Ideally, the crushable core suffers a progressive compression under a constant low stress, absorbing most of the blast induced energy and, consequently, protecting the structural element. The crushable core is commonly materialised by either a cellular solid [1-3, 7-8] or structure [9-12].

Additive manufacturing technology allows the manufacturing of complex components which would be impossible with traditional subtractive manufacturing techniques. Fused deposition modelling (FDM) is a technique based on the extrusion and is usually used in consumer-level 3D printers. This technique manufactures 3D printed parts through the layer by layer deposition of thermoplastic filaments [13]. As a result of the high manufacturing flexibility, the use of 3D printing components as energy absorption structures has grown in interest in recent years and several topologies have been studied and reported in the literature [14-16].

The present study aims to investigate the nonlinear response of 3D printed PLA honeycomb structures, both experimentally and numerically, in order to determine their energy absorption capacity when used as the crushable core of a sacrificial cladding solution. More specifically, the influence of relative density on their energy absorption capacity is verified. The response of the proposed sacrificial cladding solution is experimentally obtained resorting to an explosive driven shock tube [7], while the corresponding numerical simulations are performed using the commercial finite element software LS-DYNA [17].

EXPERIMENTAL CAMPAIGN

Crushable core samples (8×8 cm) were manufactured resorting to 3D printing as illustrated in Figure 1(a). These samples were characterized by a honeycomb structure with a height of 9 cm and two solid plates with a thickness of 2 mm, resulting in a total height of 9.4 cm. As presented in Table 1, although the wall thickness t was maintained constant, three different relative densities (5, 7.5 and 10 %) were obtained by varying the wall length l between 4.95

and 9.90 mm. It is important to refer that the 2 mm solid plates were 3D printed with the same material and parameters as the honeycomb structure.

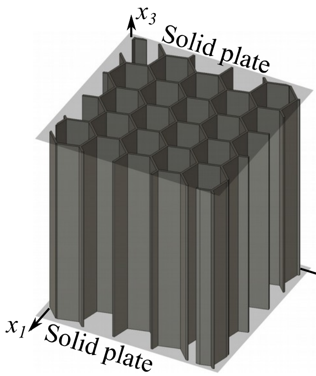

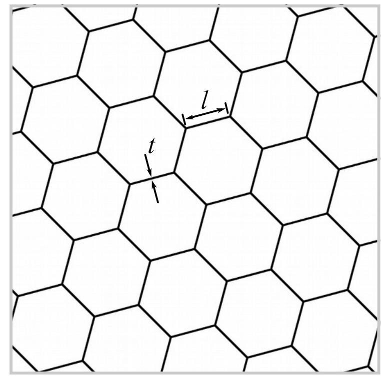

Figure 1. *Sacrificial cladding solution.*

Table 1. *Geometry of the regular hexagon honeycomb.*

Type	t [mm]	l [mm]	$\acute{\rho}[\%]$	No. of cells
1	0.43	9.90	5	5 × 5
2	0.43	6.59	7.5	7 × 7
3	0.43	4.95	10	9 × 9

Sample preparation

A Fused Deposition Modelling (FDM) 3D printer was used to manufacture the six specimens (two for each relative density) with a layer height of 0.1 mm. FDM is currently one of the most popular 3D printing technology, in which the polymeric filament (PLA in the present paper), is melted and extruded through a 0.4 mm heated nozzle that deposits the material onto a two-dimensional layer on top of another, resulting on a three-dimensional object [13]. Consequently, both the layer orientation and toolpath of depositing material influence the mechanical properties of 3D printed structures. In the present study, all the specimens were manufactured with the referred two-dimensional layers parallel to the $x_1 - x_2$ plane defined in Figure 1(a). Lastly, according to the manufacturer’s recommendations, all samples were initially deposited onto a heated bed at a temperature of 60 ºC with a nozzle temperature of 210 ºC. Based on the author’s experience, and to avoid imperfections, a printing speed of 30 mm/s was used.

Experimental set-up

The experimental campaign presented in this study, conducted in the Laboratory for the Analysis of Explosive Effects at the Royal Military Academy in Brussels, resorted to the small-scale experimental set-up depicted in Figure 2. A square section explosive driven shock tube (EDST) is used to apply a planar blast load to the specimens located at its end. This blast load results from the detonation of given explosive charge, which is positioned at definite distance from, or at, its opposite entrance [7]. As presented in Figure 2(b), the front plate of the sacrificial cladding solution, whose mass (87 g) was maintained constant throughout the entire experimental campaign, is placed at a distance of 2 mm from the end of the EDST. All the three components, the 5 mm thickness front plate, the crushable core and the 25 mm thickness rear plate, were bonded together with double-sided tape. Note that the main goal of the 3D printed solid plates was the improvement of the bond between the honeycomb structure and the referred aluminium plates. A PCB 203B force load cell is placed between the rear plate and the remainder of the set-up, whose geometry is defined in Figure 2(b), to register the transmitted load. A Photron Fastcam SA5 high speed camera was used at a frame rate of 10,000 frames per second and a resolution of 1024 by 640 pixels, resulting on an imaging magnification of 0.19 mm/pixel when measuring the displacement of the front plate. It is important to refer that all the referred measurements were synchronised by means of a light intensity trigger.

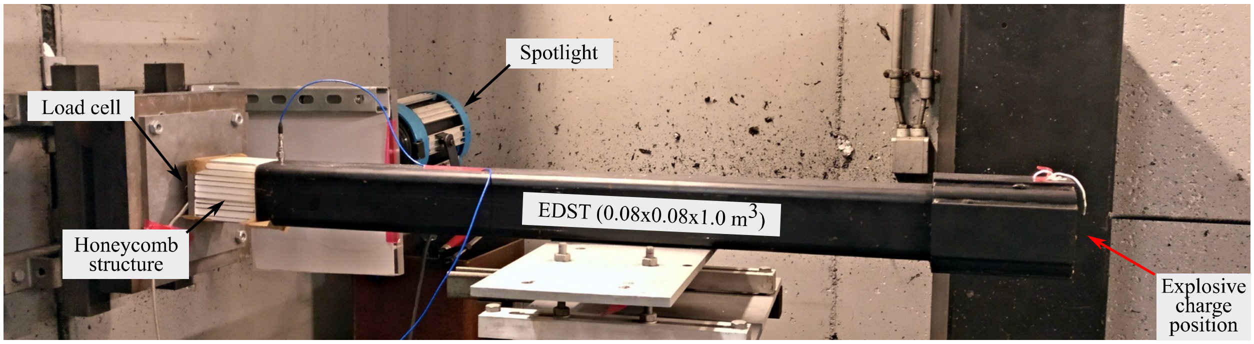

(a) Overview

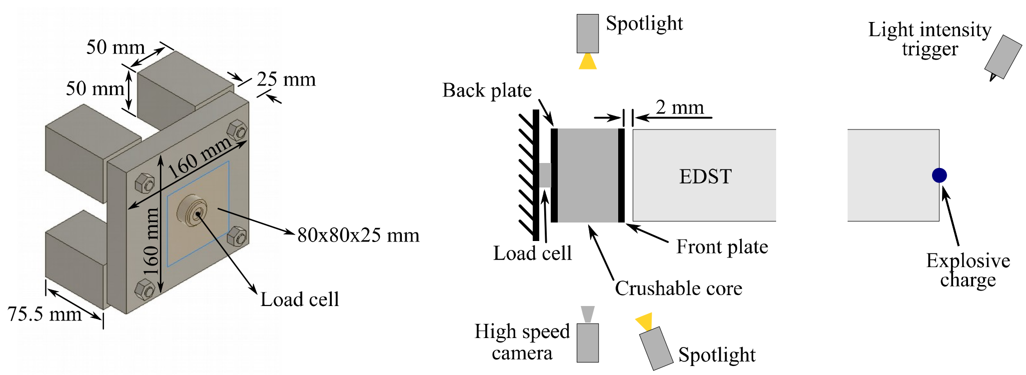

(b) Schematic representation

Figure 2. *Experimental set-up.*

Blast load on rigid and fixed boundary

Reflected pressure resulting from an explosive charge of 10 g of C4 positioned at the entrance of the EDST was measured by means of a PCB 102B pressure sensor placed centred, at 50 mm from its end. Figure 3 presents the average pressure-time history, characterised by a 20 MPa and a 2600 Pa·s reflected overpressure and impulse, respectively. The explosive charge's mass and location was maintained constant for the entire experimental campaign.

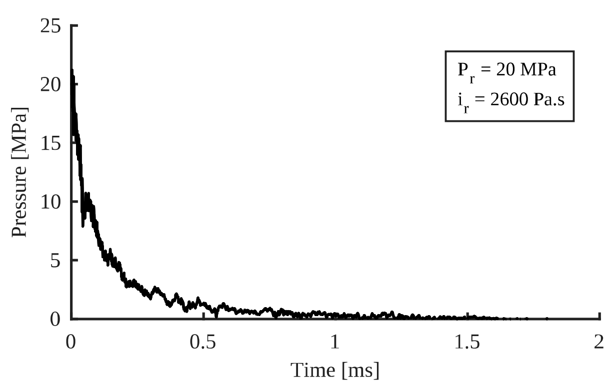

Figure 3. *Average reflected overpressure (10g of C4 at the entrance of EDST).*

NUMERICAL SIMULATION

The numerical simulations performed on the present study resort to the explicit finite element code LS-DYNA [17], using 8 nodes in parallel shared memory (double precision) of a dual Intel Xeon X670 at 2.93 GHz and 16 Gb of RAM. The time step was automatically determined by LS-DYNA, while using a scale factor of 0.6 for the computed time step, as suggested by the user manual [17].

Model description

A numerical model of the complete set-up was created in order to simulate the nonlinear response of 3D printed honeycomb structures. As illustrated in Figure 4, the PCB force sensor was modelled as a set of translational springs directly connected to the face nodes of the aluminium components. Fully integrated (`ELFORM 2`) solid elements were used on the aluminium components that were in contact with the force sensor, due to the presence of concentrated loads, while the remainder of the aluminium components was discretised with constant stress (ELFORM 1) solid elements. M10 bolts were used during the experimental campaign to fix the supports to the wall and to fix the aluminium back plate, force sensor and the remainder of the set-up. These bolts were modelled by means of spotweld beam elements (`ELFORM 9`). Lastly, the washers were simulated using Belytschko-Tsay shell elements (`ELFORM 2`) with a thickness of 2 mm.

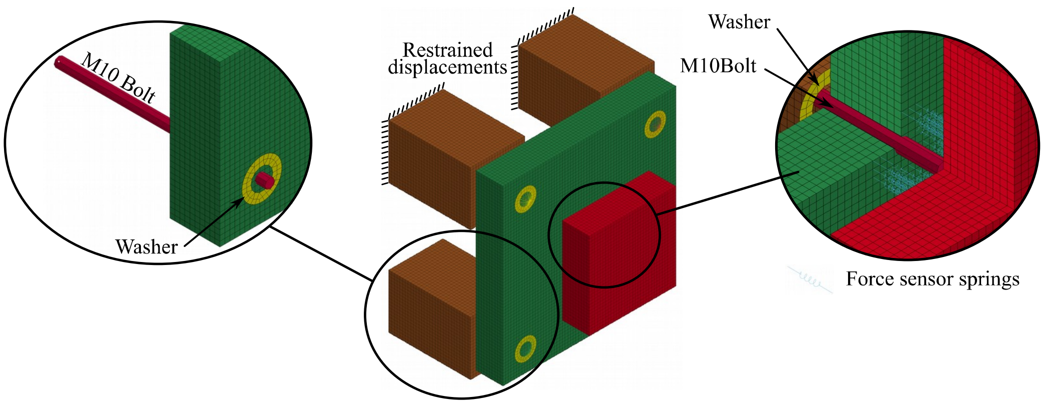

Figure 4. *FE model of the set-up.*

Both shell (crushable core) and solid (front plate) elements were used to simulate the several components of the sacrificial cladding solution, as depicted in Figure 5. The crushable core, composed by the honeycomb structure and the top and bottom solid plates, was modelled resorting to Belytschko-Wong-Chiang shell elements (`ELFORM 10`) with 5 integration points on the thickness.

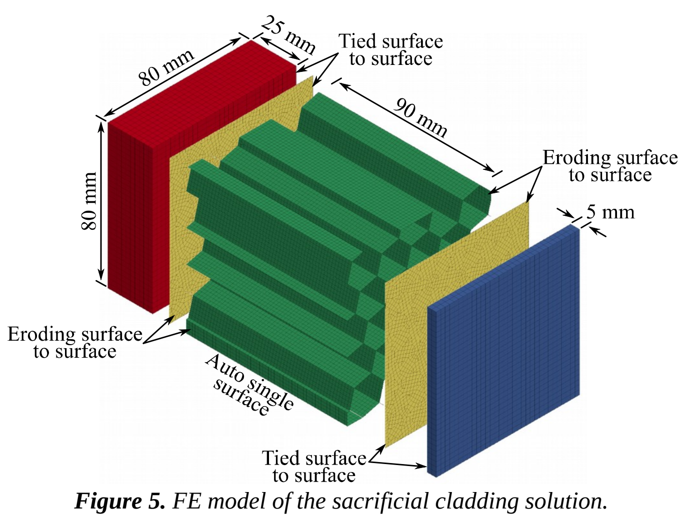

Figure 5. *FE model of the sacrificial cladding solution.*

The displacements at the end of the supports and M10 bolts, which fixed the set-up to the wall, were restrained in every direction. To guarantee the correct interaction between the simulated components, the contact algorithms presented in Figure 5 were used. Lastly, considering the geometry of the EDST, the overpressure profile depicted in Figure 3 is applied to a specific area of 75 × 75 mm^2 on the front plate via the `LOAD_SEGMENT_SET` keyword.

Material modelling

An elastic material model was used to simulate the aluminium components, the steel bolts and washers and the 3D printed top and bottom PLA plates, according to the properties defined in Table 2 and Table 3. As previously referred, the force sensor was modelled as a set of springs, which were considered as elastic with a stiffness computed as the total stiffness of the sensor, 4 kN/μm according to the sensor's specification, divided by the number of springs used in the FE model.

Table 2. *Material properties for aluminium and steel.*

Material	Density [kg/m^3]	Young's modulus [GPa]	Poisson's ratio
Aluminium	2760	72	0.34
Steel	7860	210	0.3

Table 3. *Material properties for PLA.*

Material property	Value	Unit
Density	1250	kg/m^3
Longitudinal Young's modulus	2.04	GPa
Transverse Young's modulus	2.04	GPa
Poisson's ratio	0.33	-
Longitudinal compressive strength	72.94	MPa
Longitudinal tensile strength	39.63	MPa
Transverse compressive strength	90.05	MPa
Transverse tensile strength	26.42	MPa
Shear strength	58.24	MPa

The Laminated Composite Fabric material model (MAT058) was used to model the nonlinear behaviour of 3D printed structures. On the present study, the material was considered as a unidirectional layered composite and, consequently, a smooth failure surface in the transverse direction with a limiting value in the longitudinal direction was used in the simulation. Contrary to traditional composite materials, no matrix and fibres may be explicitly defined on 3D printed materials. Nonetheless, it is considered that the material model's longitudinal direction is aligned with the 3D printing direction. Table 3 presents the complete set of properties that defines the material model, as used in the present study to simulate the nonlinear response of anisotropic PLA.

Note that, since large strains are expected in a few time steps, the LS-DYNA's user manual recommends the activation of the second order objective stress update. Additionally, the invariant node numbering for shell elements was prompted since the model possesses shells with anisotropic behaviour and element distortion is very likely.

DISCUSSION OF THE RESULTS

Preliminary tests on the experimental set-up

A preliminary set of experimental tests were conducted, on a rigid and fixed boundary, to verify the influence of the set-up on the obtained results. Figure 6 illustrates the experimental values of both the force sensor and the pressure transducer, together with the numerically simulated response of the force sensor. Spurious vibrations of the set-up are clearly visible on the force sensor's measurements (black line in the figure). Nevertheless, as expected, no energy loss was verified. Lastly, it is possible to observe that a good correlation between the experimental and numerical time histories was achieved.

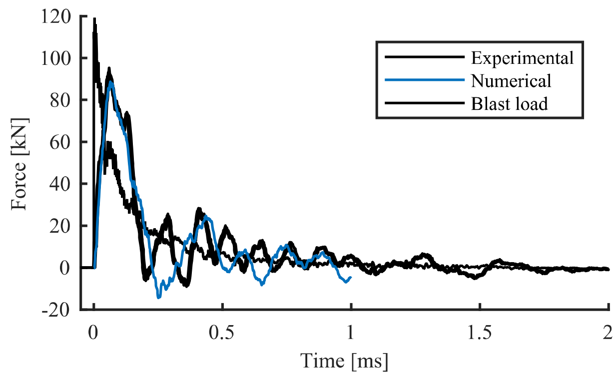

Figure 6. *Force time history on rigid and fixed boundary.*

Sacrificial cladding

The measurements obtained with the force sensor and pressure transducers during the experimental campaign (two specimens *per* $\acute{\rho}$) are illustrated in Figure 7, in combination with the numerical time history of the back plate reaction force. Analysing the referred figure, one can verify that the experimental and numerical data are in good agreement. Additionally, Figure 8 and Figure 9 present the displacement and velocity time histories, respectively, obtained by digital processing of the images recorded by the HSC (experimental) and with LS-DYNA (numerical).

Analysing the referred figures, it is possible to observe that when the blast load hits the front plate, the latter gains an initial velocity that greatly depends on the relative density, initiating a compression of the crushable core. In order to mitigate the applied blast load [1, 7], the front plate should be stopped before the densification initiation strain is reached.

The curves associated with a 5% relative density, Figure 7(a), Figure 8 and Figure 9, display a complete compaction of the honeycomb structure (90 mm maximum displacement) and an excessive secondary force peak, demonstrating that the applied blast load was not fully absorbed.

Contrarily, the proposed sacrificial cladding solution characterised by a 10% relative density only underwent partial compression, with a maximum displacement of approximately 40 mm, as depicted in Figure 8. Additionally, since no secondary peak is visible in Figure 7(c), one can conclude that the referred sacrificial cladding solution was able to fully absorb the applied blast load. Nonetheless, because the maximum displacement is significantly smaller when compared with the height of the crushable core, it is considered that the latter is oversized for the given blast load.

Lastly, analysing the plots related to a 7.5% relative density, Figure 7(b), Figure 8 and Figure 9, it is possible to verify that, although the densification phase was reached, the solution was able to stop the front plate before suffering a full compression. Therefore, the recorded secondary force peak is not as severe as the one related to the 5% relative density crushable core.

Evolution of the crushing mechanism

Resorting to the contact force between the bottom of the crushable core and the back aluminium plate obtained resorting to the numerical analysis, one may compute the stress-strain curves illustrated in Figure 10 for all relative densities. On the referred curves, several key instants were highlighted, namely the buckling of the walls (I) and the plateau region (II and III). The related deformation patterns are depicted in Figure 11. Analysing the evolution of said patterns, one may observe that their triggering and development depends on relative density. Localised crushing regions are visible for all the considered relative densities. More specifically, in the case of the 5% honeycomb structure, an increase of compression is visible for all the localised deformation regions as the nonlinear response progresses through the plateau region, culminating with the collapse of the specimen. Observing Figure 11(b), despite the presence of a third localised crushed zone at the middle of the specimen (instant III), one may conclude that the final collapsed pattern exhibits similarities when compared with the 5% solution.

Lastly, a large intact zone is visible at the core of the 10% relative density sample (see Figure 11(c)), which confirms that the solution was oversized for the applied blast load.

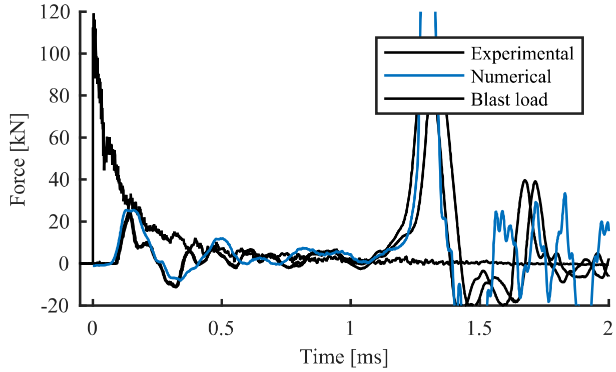

(a) 5% relative density

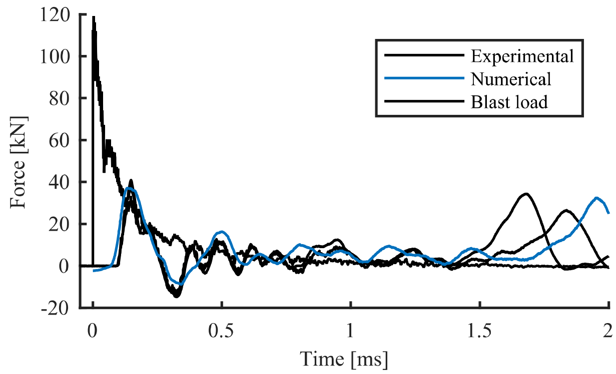

(b) 7.5% relative density

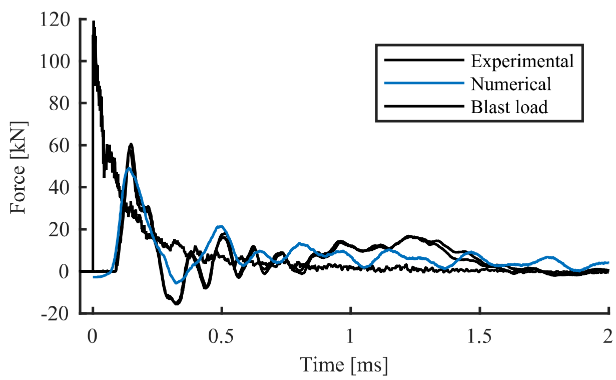

(c) 10% relative density

Figure 7. *Force time history dependence on the relative density.*

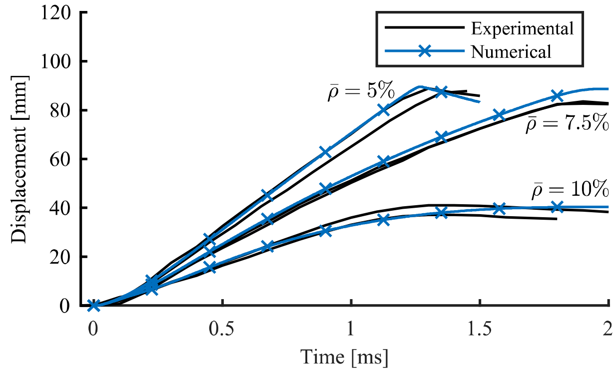

Figure 8. *Displacement time history dependence on the relative density.*

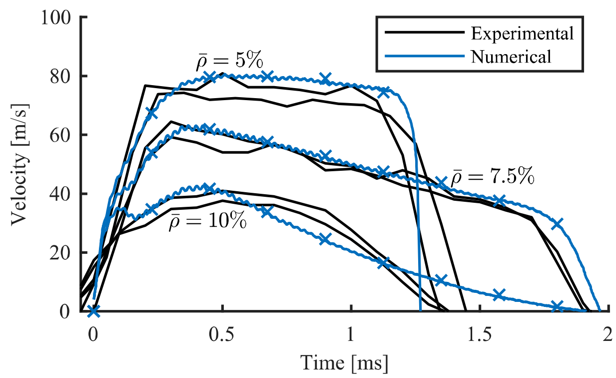

Figure 9. *Velocity time history dependence on the relative density.*

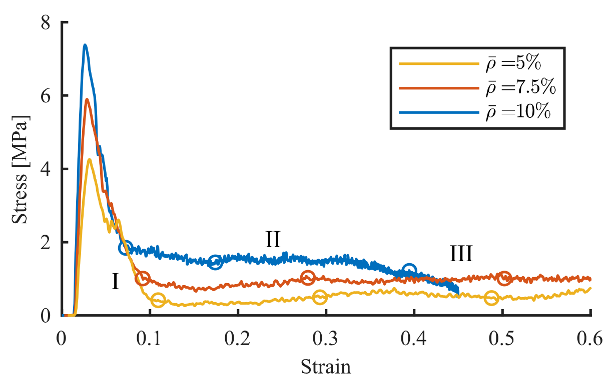

Figure 10. *Stress-strain curve dependence on the relative density.*

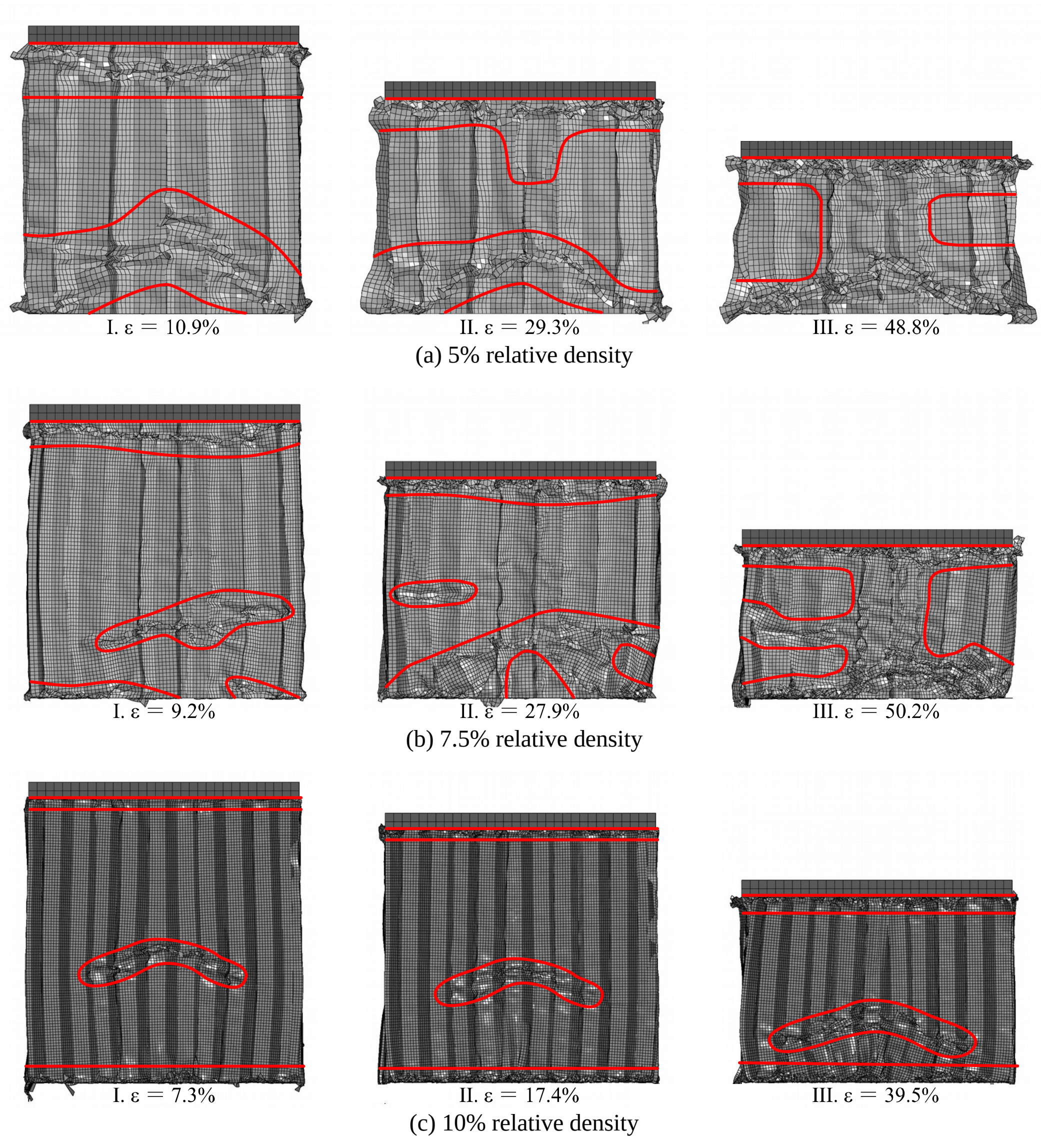

Figure 11. *Evolution of the crushing mechanism in the PLA honeycomb.*

Summary of the results

Through the analysis of the simulated contact forces depicted in Figure 10, the plateau stress (σ_{pl}), the densification initiation strain (ε_d), the transmitted energy (U_{pl}) and the energy absorbed per unit mass (SEA) were computed and presented in Table 4. The results clearly show that, when the crushable core is fully compressed, both the plateau stress and transmitted energy are proportional to the relative density. Additionally, the energy absorbed per unit mass increases with the increase of the relative density. Lastly, considering a plateau stress of 1.709 MPa and a maximum strain of 0.9, the theoretical transmitted energy becomes 860.4 J.

Table 4. *Additional numerical estimates.*

$\acute{\rho}$ **[%]**	σ_{pl} **[MPa]**	ε_d	U_{pl} **[J]**	SEA [J/g]
5	0.695	0.85	327.6	8.1
7.5	1.054	0.90	527.1	8.5
10	1.709	N.A.	416.8	10.2

CONCLUSIONS

The nonlinear response of 3D printed PLA honeycomb structures subjected to out-of-plane blast loading was determined, by means of experimental tests (EDST) and numerical simulations (LS-DYNA), in order to estimate their energy absorption capacity when used as the crushable core of sacrificial cladding solutions. The influence of the honeycomb's relative density on its nonlinear response was also verified. The findings of the present study allow to conclude that both the force peak and plateau stress are directly proportional to the relative density of the honeycomb structure More specifically, the relative density controls the crushing of the top and bottom layers and the buckling of the interior cell walls. Additionally, the results indicate that the front plate velocity also depends, not only on its mass and applied impulse, but also on the relative density of the crushable core.

ACKNOWLEDGEMENTS

This work was supported by contracts SFRH/BD/115599/2016 and PTDC/ECIEST/31046/2017 with the Portuguese funding institution FCT - Fundação para a Ciência e Tecnologia.

REFERENCES

1. Hanssen, A. G., Enstock, L., & Langseth, M. (2002). Close-range blast loading of aluminium foam panels. *International Journal of Impact Engineering*, *27*(6), 593–618.
2. Ma, G. W., & Ye, Z. Q. (2007). Analysis of foam claddings for blast alleviation. *International Journal of Impact Engineering*, *34*(1), 60–70.
3. Ye, Z. Q., & Ma, G. W. (2007). Effects of foam claddings for structure protection against blast loads. *Journal of Engineering Mechanics*, *133*(1), 41–47.
4. Ding, Y., Wang, S., Zhao, K., Zheng, Z., Yang, L., & Yu, J. (2016). Blast Alleviation of Cellular Sacrificial Cladding: A Nonlinear Plastic Shock Model. *International Journal of Applied Mechanics*, *08*(04), 1650057.
5. Lan, X. ke, Feng, S. shan, Huang, Q., & Zhou, T. (2018). Blast response of continuous-density graded cellular material based on the 3D Voronoi model. *Defence Technology*, *14*(5), 433–440.
6. Karagiozova, D., Langdon, G. S., & Nurick, G. N. (2010). Blast attenuation in Cymat foam core sacrificial claddings. *International Journal of Mechanical Sciences*, 52(5), 758–776.
7. Ousji, H., Belkassem, B., Louar, M. A., Reymen, B., Martino, J., Lecompte, D., … Vantomme, J. (2017). Air-blast response of sacrificial cladding using low density foams: Experimental and analytical approach. *International Journal of Mechanical Sciences*, 128–129, 459–474.
8. Codina, R., Ambrosini, D., & de Borbón, F. (2017). New sacrificial cladding system for the reduction of blast damage in reinforced concrete structures. *International Journal of Protective Structures*, 8(2), 221–236.
9. Tao, Y., Duan, S., Wen, W., Pei, Y., & Fang, D. (2017). Enhanced out-of-plane crushing strength and energy absorption of in-plane graded honeycombs. *Composites Part B: Engineering*, 118, 33–40.
10. Qi, C., Remennikov, A., Pei, L. Z., Yang, S., Yu, Z. H., & Ngo, T. D. (2017). Impact and close-in blast response of auxetic honeycomb-cored sandwich panels: Experimental tests and numerical simulations. *Composite Structures*, 180, 161–178.
11. Zhou, J., Guan, Z., & Cantwell, W. J. (2018). The energy-absorbing behaviour of composite tube-reinforced foams. *Composites Part B: Engineering*, 139(December 2017), 227–237.
12. Li, Z., Chen, W., & Hao, H. (2018). Numerical study of sandwich panel with a new bi-directional Load-Self-Cancelling (LSC) core under blast loading. *Thin-Walled Structures*, 127(February), 90–101.
13. Dizon, J. R. C., Espera, A. H., Chen, Q., & Advincula, R. C. (2018). Mechanical characterization of 3D-printed polymers. *Additive Manufacturing*, 20, 44–67.
14. Bates, S. R. G., Farrow, I. R., & Trask, R. S. (2016). 3D printed polyurethane honeycombs for repeated tailored energy absorption. *Materials and Design*, 112, 172–183.
15. Chen, L., Zhang, J., Du, B., Zhou, H., Liu, H., Guo, Y., … Fang, D. (2018). Dynamic crushing behavior and energy absorption of graded lattice cylindrical structure under axial impact load. *Thin-Walled Structures*, 127(October 2017), 333–343.
16. Panda, B., Leite, M., Biswal, B. B., Niu, X., & Garg, A. (2018). Experimental and numerical modelling of mechanical properties of 3D printed honeycomb structures. *Measurement: Journal of the International Measurement Confederation*, 116(July 2017), 495–506.

17. Livermore Software Technology Corporation. LS-DYNA User Manual: Volume I (Version R10.1). Livermore, CA; 2018.